

INVERSE NUMERICAL ACOUSTICS BASED ON ACOUSTIC TRANSFER VECTORS.

Michel Tournour, Luc Cremers and Pierre Guisset

LMS International
Interleuvenlaan 68,
B-3001 Leuven, Belgium
Michel.Tournour@lms.be

Fülöp Augusztinovicz and Ferenc Márki

Technical University of Budapest, Dep. of Telecommunications
Building St, Sztoczek u. 2.
H-1111 Budapest, Hungary
Fulop@hit.bme.hu

Abstract

Nearfield Acoustic Holography has proven to be a powerful tool for source identification. Nevertheless, the approach is limited to simple sources and measurement surfaces. To overcome this limitation, inverse boundary element methods are often used. A new approach based on the acoustic transfer vectors and truncated singular value decomposition is proposed here. Acoustic transfer vectors are arrays of transfer functions between surface normal velocity and acoustic pressure at response points. The approach is general and is therefore referred to as inverse numerical acoustics. So far it has been implemented using collocation and variational boundary elements. Also, apart from standard nearfield pressure measurements, the approach allows for velocity measurements on the boundary surface to increase the reliability of the source identification. It also allows for linear or spline interpolation of the acoustic transfer vectors in the frequency domain to increase computational speed. The approach will be presented together with numerical and experimental validations.

INTRODUCTION

Inverse numerical acoustics is a method which reconstructs the source surface normal velocity from a measured sound field around the source. This is of particular interest when the source is rotating or moving, too light or too hot to be instrumented by accelerometers. The use of laser vibrometers is often of no remedy due to the complex shape of the source. Unlike other nearfield acoustic holography, Inverse Numerical Acoustics can be used for any arbitrary geometry and is therefore the far most attractive alternative to plain surface velocity measurements.

Two formulations can be used to derive the integral equations: the direct formulation in terms of pressure and velocity as boundary variables and the indirect formulation in terms of single and double layer potentials (velocity jump and pressure jump respectively). The direct formulation is the most straightforward approach but the indirect formulation is the most general. Indeed, when both sides of the boundary radiate, the direct formulation fails to give a correct representation. Because it is expressed in terms of velocity jump and pressure jump, the indirect formulation is well suited to such problems. Both formulations (using a collocation technique for the direct formulation and a variational approach for the indirect formulation) will be derived in this paper.

Finally, and for sake of simplicity, the absorbent boundaries (impedance/admittance boundary conditions) and the non-uniqueness treatments will not be presented in the mathematical derivations. The reader should be aware that, although not presented, these types of boundary conditions or special treatments are possible in inverse boundary element methods.

DIRECT COLLOCATION APPROACH

Using a direct formulation, the pressure at any point of a homogeneous fluid domain containing no source can be expressed in terms of the pressure on the boundary domain and its normal derivative [1]:

$$p(\bar{x}) = \int_S p(\bar{y}) \frac{\partial G(\bar{x}|\bar{y})}{\partial n_y} dS_y - \int_S \frac{\partial p(\bar{y})}{\partial n_y} G(\bar{x}|\bar{y}) dS_y \quad (1)$$

where $p(\bar{y})$ is the pressure on the boundary and $\frac{\partial p(\bar{y})}{\partial n_y}$ its normal derivative, \bar{n}_y is the inward normal at point \bar{y} on the boundary and $G(\bar{x}|\bar{y})$ is the Green's function. Making use of the Euler equation, equation (1) becomes:

$$p(\bar{x}) = \int_S p(\bar{y}) \frac{\partial G(\bar{x}|\bar{y})}{\partial n_y} dS_y + j\rho\omega \int_S v(\bar{y}) G(\bar{x}|\bar{y}) dS_y \quad (2)$$

where $v(\bar{y})$ is the normal velocity on the boundary, ρ is the fluid mass density and ω is the angular frequency. This equation is true in the domain and on its boundary. Nevertheless, when evaluated on the boundary, the Green's function and its normal derivative become singular. Whereas the second integral of equation (2) is regular¹, the first one is singular and should be evaluated in the Cauchy's principal value sense:

$$c(\bar{x})p(\bar{x}) = P.V. \int_S p(\bar{y}) \frac{\partial G(\bar{x}|\bar{y})}{\partial n_y} dS_y + j\rho\omega \int_S v(\bar{y}) G(\bar{x}|\bar{y}) dS_y \quad (3)$$

where

¹ although regular, this integral should be evaluated using special integration schemes since the kernel is singular.

$$c(\bar{x}) = 1 + P.V. \int_S \frac{1}{4\pi|\bar{x} - \bar{y}|^2} \frac{\partial|\bar{x} - \bar{y}|}{\partial n_y} dS_y \quad (4)$$

in the three dimensional space. Note that $c(\bar{x}) = 1/2$ for a smooth surface around \bar{x} . Once discretized using boundary elements and evaluated at the mesh nodes, equation (3) leads to the following matrix system:

$$[A]\{p_b\} = [B]\{v_b\} \quad (5)$$

where the subscript b stands for *boundary*. Similarly, equation (2) gives:

$$p = \{d\}^T \{p_b\} + \{m\}^T \{v_b\} \quad (6)$$

Combining equations (5) and (6) leads to:

$$p = \{atv\}^T \{v_b\} \quad (7)$$

where $\{atv\}$ is the acoustic transfer vector, given by:

$$\{atv\}^T = \{d\}^T [A]^{-1} [B] + \{m\}^T \quad (8)$$

It is clear that the acoustic transfer vector (ATV) is an array of transfer functions between the surface normal velocity and the pressure at the field point. When the fluid domain does not exhibit any resonant behavior, the acoustic transfer vectors can be interpolated in the frequency domain using linear or spline interpolation schemes. Finally, when the pressure is evaluated at several locations, equation (7) can be rewritten as:

$$\{p\} = [ATM]^T \{v_b\} \quad (9)$$

where the acoustic transfer matrix $[ATM]$ is formed by the different acoustic transfer vectors.

INDIRECT VARIATIONAL APPROACH

Using an indirect formulation, the pressure at any point of the domain with can be expressed in terms of layer potentials [2]:

$$p(\bar{x}) = \int_S \mu(\bar{y}) \frac{\partial G(\bar{x}|\bar{y})}{\partial n_y} dS_y - \int_S \sigma(\bar{y}) G(\bar{x}|\bar{y}) dS_y \quad (10)$$

where $\sigma(\bar{y})$ and $\mu(\bar{y})$ are the single and double layer potential, respectively. For the Neuman problem and when both sides of the boundary have the same velocity, this equation can be expressed only in terms of double layer potentials:

$$p(\bar{x}) = \int_S \mu(\bar{y}) \frac{\partial G(\bar{x}|\bar{y})}{\partial n_y} dS_y \quad (11)$$

In particular, this equation can be evaluated on an arbitrary surface S' . It can be derived with respect to the normal at $x \in S'$, premultiplied by an admissible test function $\delta\mu(x)$ and integrated over the surface S' :

$$\int_{S'} \frac{\partial p(\bar{x})}{\partial n_x} \delta\mu(\bar{x}) dS' = \int_{S'} \int_S \mu(\bar{y}) \frac{\partial^2 G(\bar{x}|\bar{y})}{\partial n_x \partial n_y} \delta\mu(\bar{x}) dS_y dS'_x \quad (12)$$

Now, let the surface S' tend to S and make use of the Euler equation:

$$- \int_S j\omega\rho v(\bar{x}) \delta\mu(\bar{x}) dS = \int_S \int_S \mu(\bar{y}) \frac{\partial^2 G(\bar{x}|\bar{y})}{\partial n_x \partial n_y} \delta\mu(\bar{x}) dS_y dS_x \quad (13)$$

The right hand side integral of equation (13) contains a singularity. This singularity can be lowered down to a weak singularity using a geometrical transformation and can be evaluated using a semi-analytical integration [3] or special integration points [4]. After discretization using boundary elements equation (13) becomes:

$$p = \{d\}^T \{\mu\} \quad (14)$$

similarly, equation (13) becomes:

$$[Q]\{\mu\} = [C]\{v_b\} \quad (15)$$

Combining equations (14) and (15), we obtain:

$$p = \{atv\}^T \{v_b\} \quad (16)$$

where $\{atv\}$ is the acoustic transfer vector, given by:

$$\{atv\}^T = \{d\}^T [Q]^{-1} [C] \quad (17)$$

When the pressure is evaluated at several locations, equation (16) can be rewritten as:

$$\{p\} = [ATM]^T \{v_b\} \quad (18)$$

where the acoustic transfer matrix $[ATM]$ is formed by the different acoustic transfer vectors.

NUMERICAL ACOUSTIC HOLOGRAPHY

The proposed approach

Equations (9) and (18) are the basic relations for the inverse numerical acoustics. The pressure can be measured at a large number of field points and the boundary velocity obtained using the relationship:

$$\{v_b\} = [ATM]^{-1} \{p\} \quad (19)$$

However, the inversion of the acoustic transfer matrix is not that obvious. First, because the matrix is generally not square but rectangular. Second, because this matrix involve a Fredholm

equation (of the first kind for the indirect approach and of the second kind for the direct approach) and is ill-conditioned. Still, a pseudo-inversion can be performed and generally give good results providing that the measurement points are correctly selected. This will be treated in the following sections.

Finally, the known or measured velocities can be withdrawn from equation (18) subtracting their contribution from the measured pressure. This reduces the number of unknowns and increase the accuracy of the method.

Conditioning of the Acoustic Transfer Matrix

For a traditional Neuman problem (given velocity at the boundary surface), equations (5) and (15) are the basic equations for the boundary problem. Those equations are diagonal dominant (i.e. the dominant terms are the autoinfluences and the influences decrease with the distance) and are therefore well conditioned. Once the boundary variables are known, equations (6) and (14) are used to calculate the radiated pressure. For inverse problems, equations (6) and (14) are used to determine the boundary variables. Unfortunately, these equations are not evaluated on the boundary, the system of equations is not diagonal dominant and is generally ill-conditioned. The conditioning of the system of equations is function of the position of the field points. If the points are too far from the boundary surface, no dominant terms will appear in the acoustic transfer matrix and the later will be rank deficient, i.e. close to singular. On the other hand, if each field point is relatively close to a mesh point then its acoustic transfer vector will be dominated by this mesh point. Consequently, the acoustic transfer matrix will not be rank deficient. Still, the acoustic transfer matrix will most probably be poorly conditioned and rectangular. Therefore its inversion is performed using singular value decomposition. This point is explained in the following section.

Singular Value Decomposition

Singular value decomposition is a powerful technique to solve singular or close to singular systems. It is based on the fact that any $n \times m$ complex matrix can be written as [5]:

$$[A] = [V][\sigma][U]^H \quad (20)$$

where the superscript H stands for 'transpose complex conjugate', $[\sigma]$ is a diagonal $\min(n, m) \times \min(n, m)$ real matrix, $[U]$ is a $m \times \min(n, m)$ complex matrix and $[V]$ is a $n \times \min(n, m)$ complex matrix. The coefficients of $[\sigma]$, called singular values, are stored in an decreasing order and matrices $[U]$ and $[V]$ are such that:

$$[V]^H [V] = [U]^H [U] = [I] \quad (21)$$

From equations (20) and (21) it follows:

$$[A]^{-1} = [U][\sigma]^{-1}[V]^H \quad (22)$$

Nevertheless, singular or ill-conditioned matrices contain null or small singular values. This results in infinite or huge terms in $[\sigma]^{-1}$. Whereas the infinite terms clearly lead to an infinite solution, the huge terms lead to a solution of equation (19) that will be very sensitive to the right hand side variations. Therefore, small errors on the RHS will result in huge errors on the

solution. To avoid this problem, the small or null terms of $[\sigma]$ are set to zero in $[\sigma]^{-1}$. This process is called truncated singular value decomposition. The singular values are dropped as soon as $\sigma_i < \alpha\sigma_1$ where α is a tolerance parameter. The choice of α is a trade off between regularization and loss of information. Therefore, the critical issue of the method is to correctly select the tolerance parameter such that the errors are sufficiently reduced without causing unacceptable loss of information. Examples are shown in the coming paragraph.

EXAMPLES

Wooden box with mounted speakers

An experimental validation using a wooden box with mounted speakers has been performed. The box is 500mm wide, 500mm high and 127mm deep. Six speakers are mounted on a face of the box. Two speakers are excited using an harmonic signal at 800Hz and two other speakers are excited using an harmonic signal at 1200Hz. The pressures are measured on a plane at 70mm from the mounted speakers. The plane is 650mm wide and 650mm high. Figure (1) shows the boundary mesh and the field point mesh.

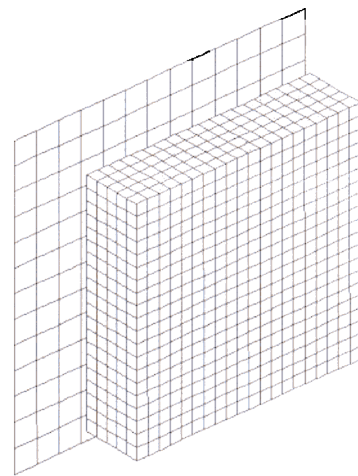


Figure 1: Boundary mesh and field point mesh

Only the front panel is supposed to be radiating, all other panels are supposed to be rigid. Figure (2) shows the retrieved boundary velocity at 800Hz and 1200Hz. The clearest picture was obtained for a tolerance α of 0.015. It can be clearly observed that only the two left speakers radiate at 800Hz and that only the two center speakers radiate at 1200Hz. It is important to note here that, although the field point mesh is not optimal and the system is underestimated, the sources are correctly detected. This shows the accuracy of the proposed technique.

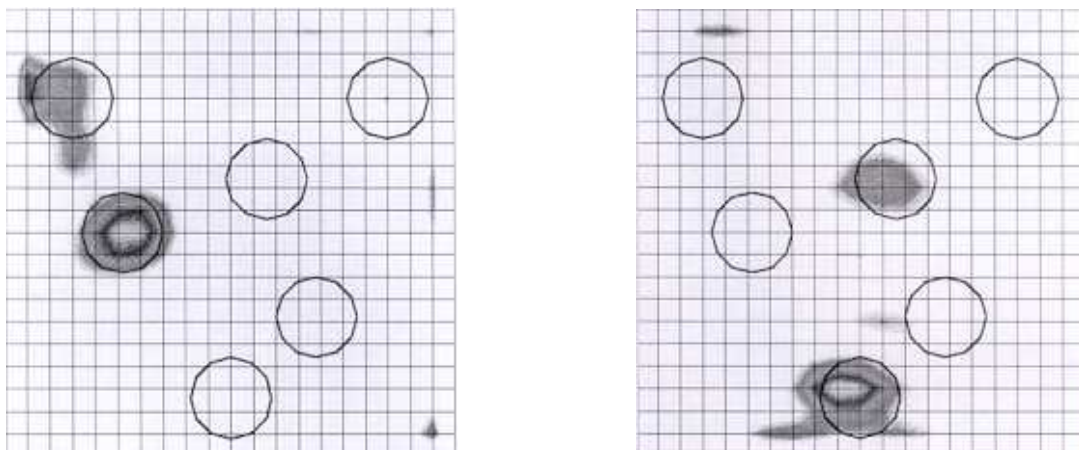


Figure 2: Retrieved velocity boundary (amplitude). Left: 800Hz. Right: 1200Hz.

Figure (3) compares the measured and calculated pressure fields at 800Hz. The calculated pressure field is obtained using the boundary velocity shown on figure (2). Note that very good agreement is found. Similar agreement is achieved for the pressure field at 1200Hz (not shown here).

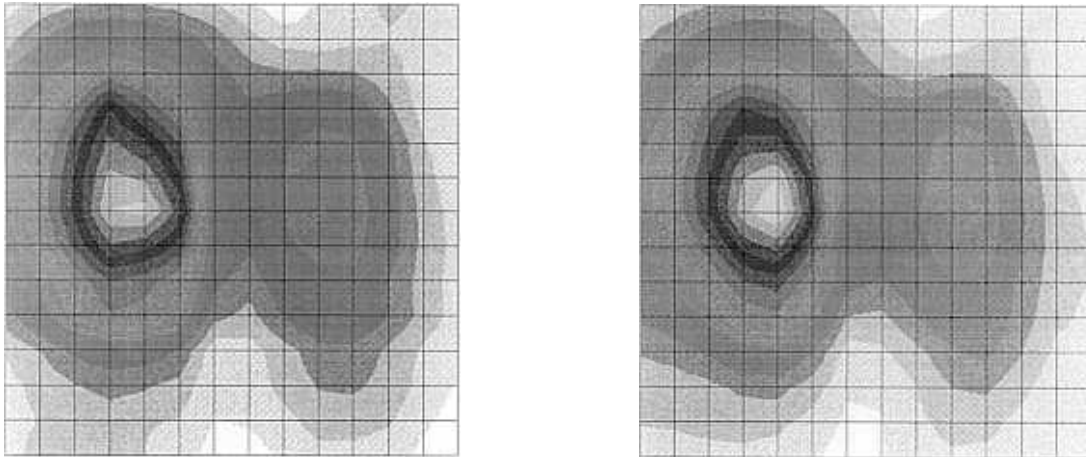


Figure 3: Field pressure at 800Hz (amplitude). Left: Measured. Right: Retrieved.

Simulated experimental results for tire noise

In order to show the accuracy of the proposed approach for arbitrary shaped sources, the analysis of tire vibrations is presented. A finite element analysis of the tire is performed in order to obtain the boundary velocities. These boundary velocities (figure 5 left) are then used to calculate the acoustic radiation and in particular the nearfield radiation (figure 4 left). The nearfield pressure is calculated only around the tread at approximately 4cm. The radiation from the tire sides is neglected. A 10% random noise is added to the nearfield calculations in order to simulate experimental results. This noise is added separately on the real and imaginary parts of the pressure in order to take into account possible errors on both amplitude and phase. Figure 4 (right) shows the simulated experimental results.

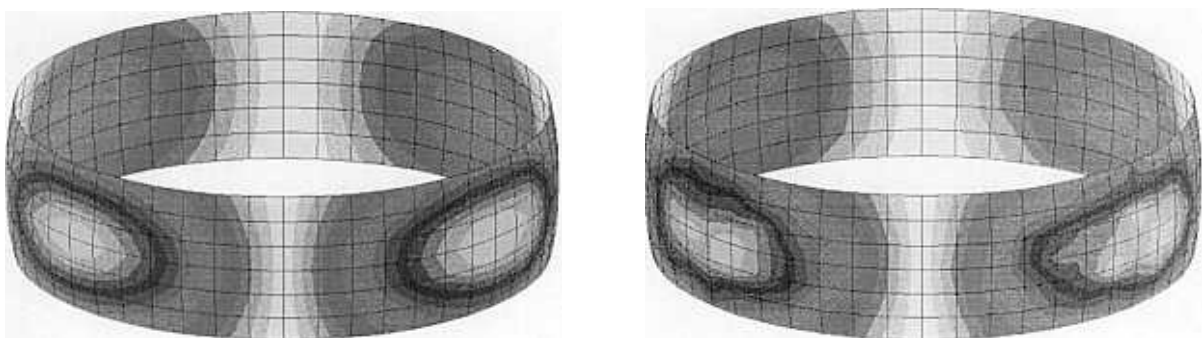


Figure 4: Nearfield pressure at 80Hz (amplitude). Left: Exact. Right: With 10% random noise.

The simulated nearfield measurements are then used to retrieve the boundary velocity using the proposed approach. Only the tire is supposed to be radiating, the central rim is supposed to be rigid. Figure 5 (right) shows the retrieved boundary velocity. The clearest picture

was obtained for a tolerance α of 0.06. It can be observed that good agreement with the original prescribed boundary velocity is obtained. Most importantly, the two radiating zones are well identified.

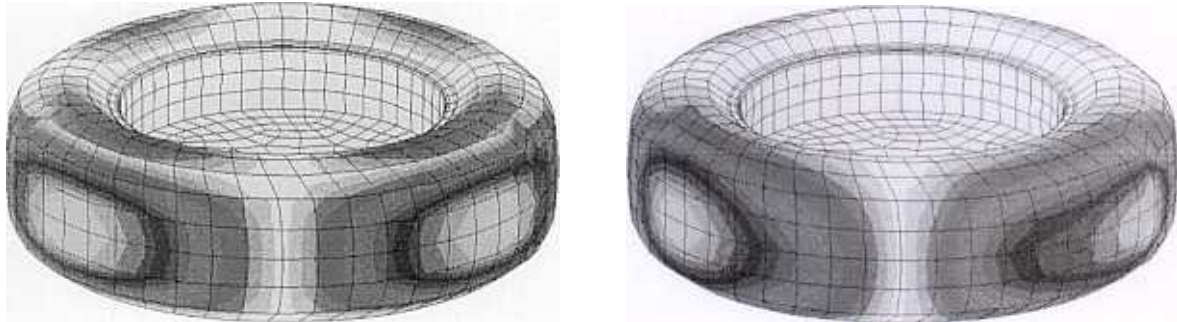


Figure 5: Boundary velocity at 80Hz (amplitude). Left: Prescribed. Right: Retrieved (with 10% random noise).

CONCLUSION

A new inverse numerical acoustics tool based on acoustic transfer vectors and truncated singular value decomposition has been presented. Acoustic transfer vectors are arrays of transfer functions between surface normal velocity and acoustic pressure at field points. Two formulations were used to obtain these acoustic transfer vectors, namely the direct collocation technique and the indirect variational approach. The approach allows for linear or spline interpolation of the acoustic transfer vectors in the frequency domain to increase computational speed. It has been shown that the method allows for an accurate reconstruction of the boundary velocity.

ACKNOWLEDGEMENTS

The presented research work was carried out in the framework of the Eureka project No 2122, BRAKE NOISE, “Methods and tools to address friction-induced noise and vibration in brakes and wheels”, supported by the Flemish Institute for the promotion of scientific and technological research in industry (IWT). The support of the Flemish government is gratefully acknowledged.

REFERENCES

- [1] H.A. Schenck, “Improved integral formulation for acoustics radiation problems”, *J. Acoust. Soc. Am.*, **44**, 41-58 (1981)
- [2] A.D. Pierce, “Variational formulations in acoustic radiation and scattering”, *Physical Acoustics*, **XXII**, 1993.
- [3] J.P. Coyette, K.R. Fyfe, “Solutions of elasto-acoustic problems using a variational finite element/boundary element technique”, *Proc. of Winter Annual Meeting of ASME, San Francisco*, 15-25 (1989).
- [4] W. Wang, N. Atalla, “A numerical algorithm for double surface integrals over quadrilaterals with $1/r$ singularity”, *Com. Num. Meth. Engng*, **13**, 885-890 (1997).
- [5] G.H. Golub, C.F. Van Loan, *Matrix Computations*. (The Johns Hopkins University Press, Baltimore and London, 1996)